# CHAPTER 4
# METHODOLOGY

## 4.1 DIFFERENTIAL SCANNING CALORIMETRY (DSC)

A heat-flux Shimadzu DSC-60A was used in this study. The measurements were carried out by monitoring the heat differential between the sample and reference material at a constant heating rate. The heat of fusion and transition temperature were calibrated using indium and tin standards. Apart from routine characterisation of different polymorphs, DSC was also used for several other analyses in this study, including investigations of $\beta$- and $\alpha$-relaxations, fragility of amorphous materials and calculation of crystalline and amorphous content. To investigate the $\beta$-relaxations, the samples were annealed well below their respective $T_g$. Under these conditions, the annealing process "unfreezes" the faster part of the relaxation spectrum (figure 4.1), which is the part predominantly associated with the $\beta$-process. The lower the temperature and the annealing time, the larger the contribution of the $\beta$-process to the overall relaxation.

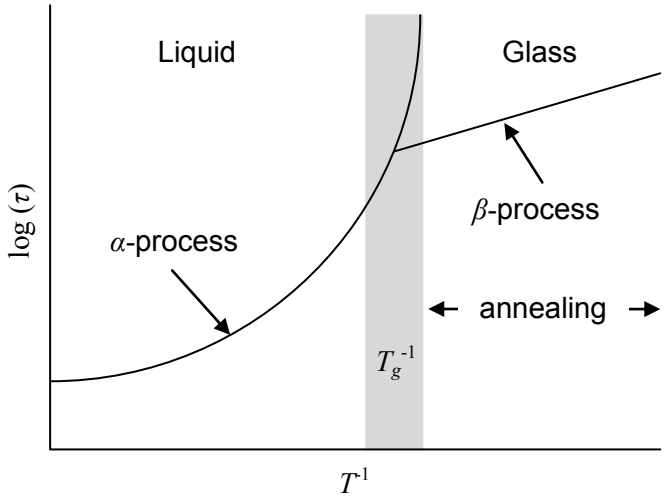


**Figure 4.1:** The relaxation spectrum of an amorphous material, showing the fast $\beta$-process, the slow $\alpha$-process and the overlapping area in the $T_g$ where these two processes couple, adapted from Vyazovkin and Dranca (2006:423).

Annealing of a glass below its $T_g$, causes it to slowly relax and lose enthalpy. When reheating the annealed glass after quick cooling, the lost enthalpy is recovered and can be

detected on the DSC as a small endothermic peak that precedes the $T_g$ (Vyazovkin & Dranca, 2006:422). At a certain temperature the $\beta$- and $\alpha$-relaxations merge as the molecular motions become more cooperative, giving rise to a broad relaxation endotherm and making accurate estimations of $\beta$- and $\alpha$-relaxations impossible. Careful determination of the annealing times and temperatures are therefore paramount to accurate investigation of $\beta$-relaxations. The activation energy of $\beta$-relaxation can then be determined from equation 4.1:

$$\frac{\Delta E}{R} = \frac{d\ln(q)}{d\left(\frac{1}{T_p}\right)} \qquad (4.1)$$

Where $\Delta E$ is the activation energy, $T_p$ is the peak temperature, $R$ is the gas constant and $q$ is the heating rate.

**Table 4.1:** The DSC traces of PVP, IM and UDA annealed at different temperatures for 30 minutes (Vyazovkin & Dranca, 2006:425)

| Compound | DSC trace |
|---|---|
| **PVP** | 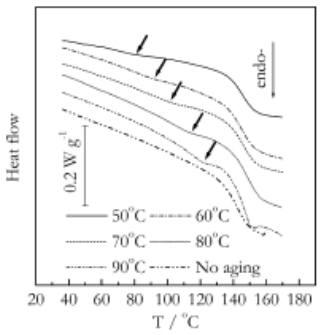 |
| **IM** | 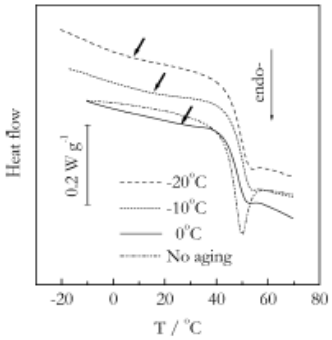 |
| **UDA** | 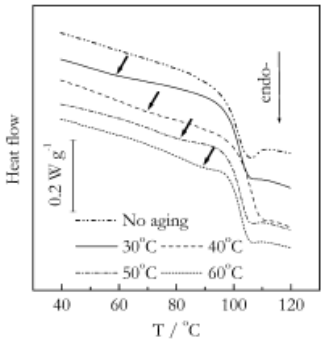 |

Equation 4.1 has values similar to dielectric and mechanical spectroscopy and has been used by Vyazovkin and Dranca (2006:422) to probe $\beta$-relaxations in poly(vinylpyrrolidone) (PVP), indomethacin (IM) and ursodeoxycholic acid (UDA). A series of annealing temperatures were chosen to determine the temperature at which the $\beta$-relaxation will be best elucidated (table 4.1). Without annealing, investigation of $\beta$-relaxations would not be possible. Vyazovkin and Dranca (2006:428) found an annealing temperature of around $0.8T_g$ to be optimal for probing $\beta$-relaxations in their study. After the optimal annealing temperature was determined, different heating rates were used to determine at which rate the $\alpha$- and $\beta$-processes would couple. This heating rate then represented the maximum rate and rates below it were used for the analysis (figure 4.2).

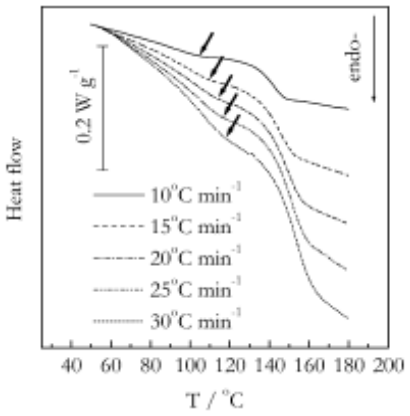


**Figure 4.2:** DSC traces obtained from different heating rates of PVP after annealing from 30 minutes at 80ºC, adapted from Vyazovkin and Dranca (2006:425).

In a similar way, the activation energy for systemic relaxation, brought on by the cooperative motions of the $\alpha$-relaxations, can be determined from equation 4.2:

(4.2)

Measurements of $T_g$ can be made either on cooling or heating of the sample, with the best reproducibility found on heating. It is absolutely essential that the heating and cooling rates be kept the same, since failure to do so will result in erroneous activation energies (Moynihan *et al*., 1974:2673; Crichton & Moynihan, 1988:413). Other requirements are that cooling must begin from well above $T_g$ and continue to well below it. Cooling and heating rates of between 2.5- to 40 K/min must be used, since cooling below these rates causes a loss in sensitivity and heating above these rates causes a significant temperature lag. With

this method, greater error is encountered when determining the $\Delta E_{Tg}$ of fragile glass formers, because of their non-Arrhenius behaviour close to $T_g$ (Crowley & Zografi, 2001:83).

Once the $\Delta E_{Tg}$ of the different glass formers are known, the fragility parameter $(m)$ can be determined, by linking $\Delta E_{Tg}$ to the VTF equation (3.3). This is done by describing the temperature dependence of the apparent activation energy $(\Delta E^*)$ across a wide temperature range in equation 4.3:

$$\frac{\quad}{\quad} \quad \frac{\tau}{\quad} \quad \frac{\quad}{\left(\quad -\right)} \tag{4.3}$$

By substituting $\Delta E^*$ with $\Delta E_{Tg}$, $m$ can be defined as:

$$\frac{\tau}{-}\Bigg| \qquad \frac{\quad}{\quad g} \tag{4.4}$$

When the minimum value of $m$ ($m_{min}$) is calculated (usually around 15), the strength parameter $D$ can be calculated using equation 4.5:

$$\frac{(\quad)}{\quad} \tag{4.5}$$

From equation 4.5 we can deduce that a large $m$ value will be the result of rapidly changing dynamics at $T_g$ which is indicative of fragile glass forming behaviour. It is also clear that $D$ is inversely proportional to $m$, a very strong glass (high $D$-value) will have a low $m$-value and a very fragile glass (high $m$-value) will have a low $D$-value.

Lefort *et al*. (2004:211) reported a convenient method of calculating the amorphous fraction ($\tau_{DSC}$) of a chemically pure compound. Their method requires the measurement of the enthalpy of crystallisation ($\Delta H_{\mathrm{cr}}$) and melting ($\Delta H_{\mathrm{m}}$) of a partially amorphous sample and the enthalpy of melting of a purely crystalline sample ($\Delta H^*_{\mathrm{m}}$). The enthalpy difference between the melting and crystallisation process for a purely amorphous system which fully recrystallises is then given by:

$$(\quad) = \quad * (\quad) - \int_{\mathrm{T}}^{\mathrm{T}} \left(\frac{\quad}{\quad}\right) - \left(\frac{\quad}{\quad}\right) \tag{4.6}$$

Where $\Delta H_{am}$ is the enthalpy of an amorphous material. However, this is a highly idealised situation, which can be easily manipulated to be more representative of an actual amorphous system. This is done by adding the variable $\tau_{DSC}$, indicating that not all of the starting material was amorphous. Furthermore, to compensate for the amorphous fraction

that does not recrystallise upon heating, the function $\alpha$ is added to the equation. Assuming that the $\Delta C_p$ between the amorphous and crystalline phases are constant in the range $T_{cr}$:$T_m$ and the melting and crystallisation do not spread over a large temperature range, equation 4.6 approximates to:

$$( \quad ) \quad \frac{( \quad )}{\tau \qquad \alpha \ ]} \tag{4.7}$$

Where $\Delta H^*_m(T_{cr})$ is the enthalpy of melting of the purely crystalline solid at the crystallisation temperature. The function $\alpha$ depends on the stability properties of the amorphous fraction as well as the heating protocol, but is independent on $\tau$, and is obtained by equation 4.8:

$$\alpha \quad \frac{( \quad )}{( \quad )} \tag{4.8}$$

So the $\tau_{DSC}$ can be directly derived from equation 4.9:

$$\tau \quad \frac{( \quad )}{( \quad )} \frac{}{\alpha} \tag{4.9}$$

One of the advantages of this method of determining the amorphous fraction is based on first principles and does not require a calibration curve (Shah *et al*., 2006:1646). The effect of amorphous content on DSC thermograms can be seen in figure 4.3.

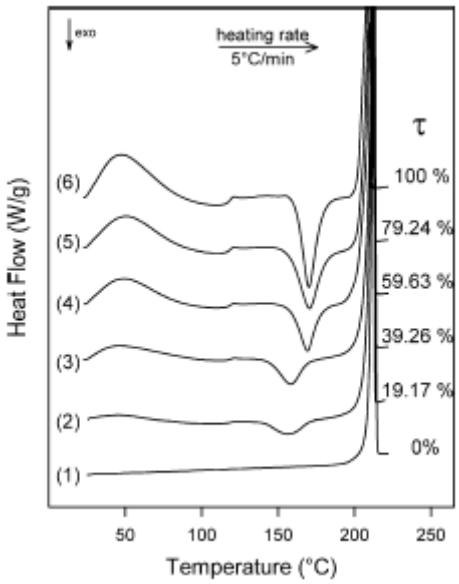


**Figure 4.3:** DSC thermograms of trehalose containing varying degrees of amorphous content, adapted from Lefort *et al*. (2004:212).

## 4.2 THERMOGRAVIMETRIC ANALYSIS (TGA)

TGA is the measure of the thermally induced weight loss of a material as a function of the applied temperature. Although TGA is restricted to transitions characterised by an increase or decrease in mass, it is very useful when combined with Karl Fischer (KF) titrations or a DSC. When used as an adjunct to a KF titration, distinction can be made between solvates and hydrates of a certain compound. In the case of binary solvent mixtures containing water, it can also enable us to quantify the amount of water in the total weight loss. When used adjunct to a DSC the TGA can be used to distinguish between thermal events, for example desolvation processes which are accompanied by weight loss and solid-solid phase transitions which are not.

TGA in this study was performed on Shimadzu DTG-60. The temperature functions were calibrated with indium and tin standards. Apart from its use supplementary to DSC and KF, the TGA is also a powerful tool in its own right, especially when working with solvates or hydrates, as its enables the researcher to calculate the stoichiometry between the solvent and drug molecules through equation 4.10:

$$(\quad) \quad \frac{\qquad\qquad\qquad\qquad}{(\qquad)} \; x \qquad (4.10)$$

This stoichiometric data is of great importance, specifically for single crystal X-ray diffraction (SXRD) where it helps the researcher elucidate the origin of extra atoms found in the unit cell.

## 4.3 KARL FISCHER TITRATION (KF)

The water content of crystals believed to be hydrates were obtained from binary solvent mixtures was determined with a Metrohm 870 KF Titrino Plus. Accurately weighed samples (100 mg) were dissolved in methanol and the water content was titrated using hydranal.

## 4.4 FOURIER TRANSFORM INFRARED SPECTROSCOPY (FTIR)

A Shimadzu IRPrestige-21 was used in this study. The wavelengths were checked with polystyrene film and the machine was validated according to the European Pharmacopoeia's standards. Spectra were recorded over a range of 500 – 4000 $cm^{-1}$. KBr was used as

background and the samples were homogeneously dispersed in a ground matrix of KBr powder prior to analysis.

Of particular interest to the pharmaceutical scientist is the ability of the FTIR machine to give vibrational data of the solid-state. Although most functional groups have characteristic IR absorption bands, FTIR can be used quite effectively to investigate solid-state properties of pharmaceuticals. Because of the quantised nature of molecular energy, changes in bond length will have a direct influence on the frequency at which molecules stretch or bend, which in turn determines at which frequency the molecule will absorb electromagnetic radiation. Changes in bond length can be seen as peak shifts in the wavenumber on an interferogram.

This method has been used for decades and an example can be found in the work of Curtin and Byrn (1969:1865) who investigated the stereoisomerism of dimethyl 3,6-dichloro-2,5-dihydroxyterephthalate, which exists as either white or yellow crystals at room temperature, using infrared and $^{35}Cl$ nuclear quardupole resonance spectroscopy. The results showed a sharp carbonyl peak at 1666 $cm^{-1}$ for the yellow crystals and a peak at 1700 $cm^{-1}$ for the white crystals. The absence of any other absorption between 1500 and 1800 $cm^{-1}$ for the yellow crystals, along with a broad OH stretch at 3100 $cm^{-1}$, was consistent with that of a hydroxyl ester structure. Hydrogen bonding between the carbonyl oxygen and adjacent hydroxyl groups on the same molecule could account for the differences in absorption between the molecules in the yellow and white crystals. Their conclusion was that the yellow crystals contained strong intramolecular hydrogen bonds, while the white crystals contained weaker intermolecular hydrogen bonding (figure 4.4). These results were later confirmed by single crystal X-ray diffraction.

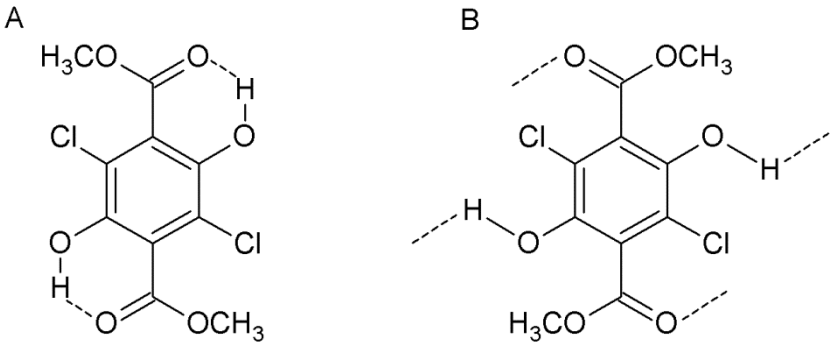


**Figure 4.4:** The chemical structures of dimethyl 3,6-dichloro-2,5-dihydroxyterephthalate in the yellow (A) and white (B) crystals (Curtin and Byrn, 1969:1865).

The degree of crystallinity can also be determined from whole-spectrum FTIR scans by identifying peaks which are depend and independent on crystallinity. This method was used by Black and Lovering (1977:686) to estimate the degree of crystallinity in digoxin (figure 4.5).

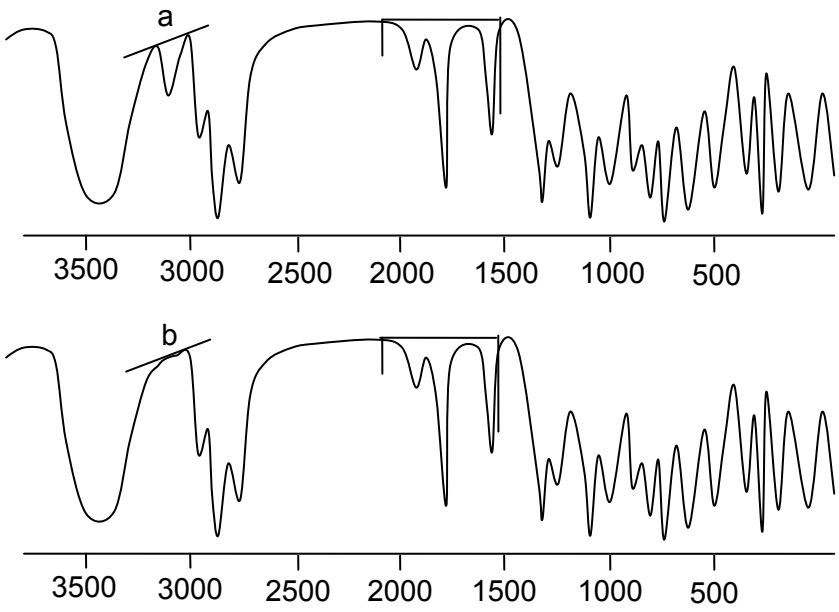


**Figure 4.5:** Infrared spectra of crystalline (a) and amorphous digoxin (b), adapted from Black and Lovering (1977:686).

To determine the percentage crystallinity, the heights of the peaks were measured by extrapolating base lines between the minima at 3050 and 3150 $cm^{-1}$ and between 1550 and 1900 $cm^{-1}$. The ratios of the crystalline to independent peaks were then plotted against mixtures of crystalline and amorphous digoxin (in known percentages) and those with the best fit were chosen as the working ratios. The percentage crystallinity of an amorphous digoxin preparation was then read off the graph, based on its crystalline to independent peak ratio.

## 4.5 ULTRAVIOLET ABSORPTION SPECTROPHOTOMETRY (UV)

A Shimadzu UV-1800 was used for all UV absorbance measurements in this study. In accordance with the Beer-Lambert law, UV absorbance was used to determine the concentration (and hence the maximum solubility) of the different polymorphs and glasses prepared in this study. Calibration traces were drawn from the raw materials over a wide

concentration range, in triplicate and at the desired temperature (310 K) for each of the solvents used in the solubility study.

## 4.6 HOT STAGE MICROSCOPY

A Nikon Eclipse E400 microscope fitted with a heating stage was used in this study. The microscope was equipped with a Nikon DS-Fi1 camera and the temperature was monitored using a Goerz Metrawatt BBC Metratherm 1200d thermometer. The microscope was also equipped with a polarised light filter, which allows the observer to differentiate between amorphous and crystalline components in the same system. Thermomicroscopy was also used supplementary to DSC and TGA to visually confirm thermal events, for example, the escape of solvent during desolvation.

## 4.7 POWDER X-RAY DIFFRACTION (PXRD)

PXRD data was obtained from a PANalytical X'Pert Pro from continuous scanning runs at room temperature. Measurement conditions were: Anode material, Cu; Generator settings, 40 mA, 45 kV; divergence slit, 0.957°, fixed; step size, 0.017° in $2\theta$; scan step times, 19.685 s. The samples were rotated during scans to minimise preferred orientation, which was absolutely essential considering the morphological nature of the obtained Didanosine crystals (see next chapter). In cases where the crystals were believed to be solvates, the crystals were ground under mother liquor to minimise solvent loss.

Although Bragg's Law gives us the scattering angles with regard to the incident X-ray beam, it is through Thompson's Law on the scattering by an electron that we are able to use the relative intensities on a diffractogram to derive additional information concerning a crystallite. Black and Lovering (1977:684) calculated the percentage crystallinity ($X_{cr}$) using equation 4.11:

$$= \frac{\text{x}}{+} \qquad (4.11)$$

Where $I_c$ and $I_a$ are the intensities of X-rays scattered from the crystalline and amorphous regions respectively. Apart from working with the peak intensities, the ratios ($R_x$) of the areas under the diffraction peaks to the total area can also be used by plotting these $R_x$ values against mixtures of known crystalline and amorphous percentages digoxin. The degree of crystallinity was then calculated using equation 4.12:

$$C = R_x \text{ x } 100 \quad (4.12)$$

Equation 4.12 predicts a linear relation between the degree of crystallinity and $R_x$, which Black and Lovering (1977:685) found to be true. Saleki-Gerhardt *et al*. (1994:237) used PXRD to calculate the percentage amorphous content from equation 4.13:

$$\%Disorder = 100 - [(X - X_a)/(X_c - X_a)] \text{ x } 100 \quad (4.13)$$

Where $\%Disorder$ is the percentage amorphous content (disorder refers to the randomness of molecular conformation in the amorphous state), $X$ is the area under the curve measured for the sample and $X_a$ and $X_c$ are the areas under the curve for completely amorphous and crystalline samples respectively. It is well known that variations in particle size and lattice strain can significantly influence the line shape in PXRD, however, by integrating the peak intensities these variables will not be reflected in the final result, adding to the appeal of this method for calculating the $\%Disorder$ (Shah *et al*., 2006:1645).

## 4.8 SINGLE CRYSTAL X-RAY DIFFRACTION (SXRD)

To elucidate the molecular packing in the unit cells of the crystals obtained, X-ray intensity data was collected on a Bruker Apex Duo diffractometer.

## 4.9 SCANNING ELECTRON MICROSCOPY (SEM)

To investigate the morphologies of the crystals prepared in this study, SEM was employed. SEM micrographs were taken using a FEI Quanta 200 ESEM. Measurement conditions: Voltage, 10 kV; vacuum, high and low depending on the nature of the individual analysis, coating, Au/Pd to a thickness of 20 nm.

## REFERENCES

BLACK, D.B. & LOVERING, E.G. 1977. Estimation of the degree of crystallinity in digoxin by X-ray and infrared methods. *Journal of pharmacy and pharmacology*, 29:684-687, Apr.

CRICHTON, S.N. & MOYNIHAN, C.T. 1988. Dependence of the glass transition temperature on heating and cooling rate. *Journal of non-crystalline solids*, 99(2-3):413-417, Feb.

CROWLEY, K.J. & ZOGRAFI, G. 2001. The use of thermal methods for predicting glass-former fragility. *Thermochimica acta*, 380:79-93.

CURTIN, D.Y. & BYRN, S.R. 1969. Stereoisomerism at the oxygen-carbon single bond due to hydrogen bonding. Structures of the Yellow and White Crystalline Forms of dimethyl 3,6-dichloro-2,5-dihydroxyterephthalate, *Journal of the American Chemical Society*, 91(7):1865-1866, Mar.

LEFORT, R., DE GUSSEME, A., WILLART, F.-J., DANèDE, F. & DESCAMPS, M. 2004. Solid state NMR and DSC methods for quantifying the amorphous content in solid dosage forms: an application to ball-milling of trehalose. *International journal of pharmaceutics*, 280:209-219, May.

MOYNIHAN, C.T., EASTEAL, A.J., WILDER, J. & TUCKER, J. 1974. Dependence of the glass transition temperature on heating and cooling rate. *The journal of physical chemistry*, 78(26):2673-2677, Dec.

SALEKI-GERHARDT, A., AHLNECK, C. & ZOGRAFI, G. 1994. Assessment of disorder in crystalline solids. *International journal of pharmaceutics*, 101(3):237-247, Jan.

SHAH, B., KAKUMANU, V.K. & BANSAL, A.K. 2006. Analytical techniques for quantification of amorphous/crystalline phases in pharmaceutical solids. *Journal of pharmaceutical sciences*, 95(8):1641-1665, Aug.

VYAZOVKIN, S. & DRANCA, I. 2006. Probing beta relaxation in pharmaceutically relevant glasses by using DSC. *Pharmaceutical research*, 23(2):422-428, Feb.